haematologica
Journal of the Ferrata Storti Foundation

Checkpoint inhibition enhances cell contacts between CD4+ T cells and Hodgkin-Reed-Sternberg cells of classic Hodgkin lymphoma

by Kübra Yadigaroglu, Sonja Scharf, Steffen Gretser, Hendrik Schäfer, Aresu Sadeghi Shoreh Deli, Andreas G. Loth, Hasmik Yegoryan, Roland Schmitz, Emmanuel Donnadieu, Martin L. Hansmann, and Sylvia Hartmann

Received: December 6, 2023.
Accepted: May 16, 2024.

Citation: Kübra Yadigaroglu, Sonja Scharf, Steffen Gretser, Hendrik Schäfer, Aresu Sadeghi Shoreh Deli, Andreas G. Loth, Hasmik Yegoryan, Roland Schmitz, Emmanuel Donnadieu, Martin L. Hansmann, and Sylvia Hartmann. Checkpoint inhibition enhances cell contacts between CD4+ T cells and Hodgkin-Reed-Sternberg cells of classic Hodgkin lymphoma. Haematologica. 2024 May 23. doi: 10.3324/haematol.2023.284512 [Epub ahead of print]

Checkpoint inhibition enhances cell contacts between CD4$^+$ T cells and Hodgkin-Reed-Sternberg cells of classic Hodgkin lymphoma

Kübra Yadigaroglu[1], Sonja Scharf[1,2], Steffen Gretser[1], Hendrik Schäfer[1], Aresu Sadeghi Shoreh Deli[3], Andreas G. Loth[3], Hasmik Yegoryan[4], Roland Schmitz[4], Emmanuel Donnadieu[5], Martin-Leo Hansmann[6,7], Sylvia Hartmann[1]

[1] Dr. Senckenberg Institute of Pathology, Goethe University Frankfurt am Main, Theodor-Stern-Kai 7, D-60590 Frankfurt a. Main, Germany

[2] Molecular Bioinformatics, Goethe University Frankfurt am Main, Robert-Mayer-Str. 11-15, 60325 Frankfurt am Main, Germany

[3] Department of Otolaryngology, Head and Neck Surgery, University Hospital Frankfurt, Frankfurt am Main Germany

[4] Department of Pathology, Justus Liebig University Giessen, Giessen Germany

[5] Universite´ Paris Cité, CNRS, INSERM, Equipe Labellisée Ligue Contre le Cancer, Institut Cochin, 75014 Paris, France

[6] Frankfurt Institute for Advanced Studies, Ruth-Moufang-Str. 1, 60438 Frankfurt am Main, Germany

[7] Institute of General Pharmacology and Toxicology, Goethe University Frankfurt am Main, Theodor-Stern-Kai 7, D-60590 Frankfurt a. Main, Germany

Running title: Effects of Nivolumab on native Hodgkin lymphoma tissue

Key words: Nivolumab, check point inhibition, classic Hodgkin lymphoma, hyperplastic lymphoid tissue, live cell imaging, cell-cell contacts

Corresponding author:
Sylvia Hartmann, MD
Dr. Senckenberg Institute of Pathology
Goethe University Frankfurt
Theodor-Stern-Kai 7
D- 60590 Frankfurt am Main, Germany
Phone: +49-69-6301-4284 Fax: +49-69-63015241
Mail: s.hartmann@em.uni-frankfurt.de

Conflict of interest

The authors do not report any conflict of interest.

Acknowledgements

We thank Yvonne Steiner and Vivienne van Oostendorp for excellent technical assistance. We thank Prof. Ralf Küppers, Essen, and Julia Bein, Frankfurt for helpful discussions. We thank Prof. Matthieu Piel, Institut Gilles de Gennes, Paris, for providing microfluidic moulds for microchannels and helpful discussions. S.H. is supported by the Deutsche Forschungsgemeinschaft (HA6145/6-1 and HA6145/7-1).

Author contributions

KY: performed research, data analysis, interpreted data, wrote manuscript; SS, SG; HS, ASSD, AGL: performed research, contributed essential material, data analysis, interpreted data, critically revising the manuscript; ED, MLH, HY, RS: data interpretation, contributed essential material, critically revising the manuscript; SH: concept of study, acquisition of funding, data analysis, interpreted data, wrote manuscript

Data Availability Statement

Imaging data are available from the corresponding author on reasonable request.

Funding

This project was supported by the Deutsche Forschungsgemeinschaft (grants HA6145/6-1 and HA6145/7-1).

Abstract

Although checkpoint molecules like CTLA-4 and PD1 have been described several years ago, checkpoint inhibitors such as Nivolumab (an anti-PD-1 antibody) have only recently been used to treat classic Hodgkin lymphoma (cHL). Several studies have shown convincing therapeutic effects of Nivolumab in cHL. However, the mechanism of action of Nivolumab in cHL is not fully understood.

The aim of this study was to monitor changes in cell motility and cell contacts after administration of Nivolumab to an *in vitro* model of cHL as well as to native hyperplastic lymphoid tissue and native human tissue from cHL. In both tissue and *in vitro*, $CD4^+$, $CD8^+$, $CD30^+$ and $CD20^+$ cell velocities were unchanged after Nivolumab incubation. In contrast, in primary cHL tissue, the duration of cell contacts between $CD4^+$ T cells and HRS cells was significantly increased after 5 h Nivolumab treatment, and the number of contacts with HRS cells was also slightly increased for $CD4^+$ T cells (not significant), suggesting that $CD4^+$ T cells in particular contribute to the cytotoxicity observed as a result of Nivolumab therapy. There was no change in the duration of cell contacts in the hyperplastic lymphoid tissue after Nivolumab incubation. In conclusion, we show here for the first time by imaging of native lymphoma tissue an enhanced interaction of $CD4^+$ T cells and HRS cells in cHL after Nivolumab administration.

Introduction

The human immune system is a sophisticated structure that controls most types of infectious agents as well as developing malignant cells. However, on relatively rare occasions malignant cells manage to escape this highly efficient control system, leading to the development of a neoplasm. The first immune checkpoints, such as CTLA-4 and PD1, were discovered 20 years ago.[1-3] It is only in recent years that therapies targeting these specific checkpoints have been developed. Checkpoint inhibitors are very effective, especially in tumors with a high mutational burden and expression of tumor-specific neo-antigens.[4] Among lymphoid-derived tumours, classic Hodgkin lymphoma (cHL) is a neoplasm that often shows a good outcome after checkpoint inhibitor therapy.[5-11] Patients with de novo early unfavourable cHL showed an overall survival rate of 100% after a median follow-up of 41 months in the NIVAHL trial.[8] However, the exact mechanism that leads to the dissolution of HRS cells remains so far unknown.

To exert their anti-tumour activity, T cells must form a productive conjugate with their targets. In solid tumours, an inability of T cells to migrate and reach cancer cells has been described resulting in an "immune-excluded" tumour profile, which may explain why anti-PD1 antibodies do not always give the expected results.[12] Although T cell motility is a critical factor influencing the success of immunotherapy, there is limited experimental data exploring the potential links between PD1 blockade and T cell migration, particularly in a tumour context.

In vitro co-culture experiments provided the first evidence that PD1 controls T cell motility and interaction time between T cells and antigen-presenting cells.[13,14] In brief, it has been demonstrated that engagement with PD1 reduces TCR-induced signalling, thereby preventing T cells from establishing stable contact with antigen-presenting cells. Conversely, when PD1 binding to its ligand was blocked, T cells were able to regain stable contact with antigen-presenting cells. Intravital two-photon microscopy of a murine melanoma model showed that PD1 blockade restored stabilized conjugates between T cells and tumour cells.[15]

As the efficacy of Nivolumab in the treatment of cHL has now been demonstrated in multiple studies, the aim of the present study was to further elucidate the direct effect of

Nivolumab on $CD4^+$ and $CD8^+$ lymphocytes, under reactive/inflammatory conditions and in cHL.

Methods

In vitro model

For the cHL *in vitro* model, the cHL cell lines L-428 (CVCL_1361) and L-1236 (CVCL_2096) were purchased from DSMZ (Braunschweig, Germany). Cell lines were transduced to express Life-Act GFP as previously described[16] for a better visualization in microfluidics microchannels.

$CD4^+$ and $CD8^+$ T cells were purified from peripheral blood by magnetic activated cell sorting (MACS) using the untouched $CD4^+$ and $CD8^+$ T cell Isolation Kits (Miltenyi Biotec, Bergisch-Gladbach, Germany). The purity of the isolated cells was confirmed by FACS to be > 94% for $CD4^+$ T cells (CD4-Vioblue antibody, Miltenyi Biotec) and > 89% for $CD8^+$ T cells (CD8-PE/Cy7-antibody, Clone SK1, Biolegend, San Diego, CA, USA). T cells were either kept in culture overnight with IL-2 supplementation to recover from the MACS procedure or activated with dynabeads human T-Activator CD3/CD28 (Gibco, Thermofisher Scientific, Waltham, MA, USA) for 48 hours and then seeded at 2 x 10^5 cells in a microchannel punch. Nivolumab or an IgG4 kappa isotype control antibody (MedChemExpress, Monmouth Junction, NJ, USA) was added at a dose of 10 µg/ml to the cell culture medium that was used to resuspend the cells. The other punch on the opposite side of the 4 x 10 µm microchannels was loaded with 2 x 10^7 cells of either L-428 or L-1236 cell lines (see Fig. 1A). Time-lapse images were taken every 4 min overnight. The velocity of the cells was measured as previously published.[16] The duration and number of cell-cell interactions was manually analyzed. To assess the expression of immune checkpoint proteins on activated T cells, T cells were cocultured overnight with the L-1236 cell line or an L-1236 PD-L1 knockout cell line at a ratio of 20:1. The expression of PD1, LAG-3, TIM-3 and TIGIT before and after coculture was determined by flow cytometry (Suppl. Methods).

Suggestions for text editing were generated by artificial intelligence (DeepL). All suggestions were checked by the authors for accuracy.

Live cell imaging

For 4D imaging, thick sections from thirteen cases of hyperplastic lymphatic tissue from the pharyngeal tonsil and six cases of cHL were analysed as previously described.[17] CHL cases 1-3 and 6 were nodular sclerosing subtype and EBV-negative, the 4th and 5th case were EBV-positive mixed cellularity (Suppl. Table 1). From the 5th case only movies in the untreated condition could be obtained due to limited tissue size.

The study was conducted according to the declaration of Helsinki and informed consent was obtained from all patients. The ethic committee of Goethe University Hospital agreed on the study (Nr20-376aV). The tissue was stained with fluorescent antibodies against CD4 (T helper cells, clone SK3, NovaFluor Blue 585, ThermoFisher Scientific), CD8 (Cytotoxic T lymphocytes, clone SK1 AlexaFluor 647, Biolegend), CD20 (B cells, Clone L26, AlexaFluor 488, ThermoFisher Scientific), and CD30 (Clone BerH2, sc-19658 AF488, Santa Cruz Biotechnologies, Santa Cruz, CA, USA). In each case, Nivolumab was added at a dose of 100 µg/ml on top of the tissue slices and then overlayed with RPMI medium. In the cases of hyperplastic lymphoid tissue an IgG4 kappa isotype antibody was added as negative control in addition to the untreated condition.

Results

CD4$^+$ resting T cells show prolonged cell contacts with cHL cell line L-1236 in microfluidic microchannels after incubation with Nivolumab

To model the effects of Nivolumab on T cells and HRS cells, we first used a model system with microfluidic microchannels, where the different cell types (i.e. T cells vs. HRS cells) can enter the microchannels from opposite sides (Figure 1A). cHL cell lines L-428 and L-1236 were used, which both show expression of PD-L1 (Figure 1B) and loss of expression of major histocompatibility complex (MHC) class I (L-428) or II (L-1236, Suppl. Figure 1) as frequently observed in HRS cells in primary cHL cases.[18] In general, activated T cells moved at a higher velocity (means 3.51 - 5.01 µm/min, Figure 1D) when compared with resting T cells (means of 1.93 - 4.3 µm/min Figure 1C). There

was no systematic difference in velocity when either Nivolumab or the IgG4 kappa isotype control antibody was added to the cell culture medium.

The duration of cell-cell contacts with HRS cells of the L-1236 cell line was significantly increased for resting $CD4^+$ T cells in the presence of Nivolumab when compared to the IgG4 kappa isotype control (mean of 96.00 vs. 15.64 min, Figure 1E, G and H, $p<0.01$, Kruskal-Wallis-test). In addition, contacts with activated $CD8^+$ T cells were significantly longer compared to the IgG4 kappa isotype control (mean of 121.00 vs. 15.84 min, Suppl. Figure 2, $p<0.01$, Kruskal-Wallis-test). In the L-428 cell line there was no effect of Nivolumab treatment on the duration of cell-cell contacts (Figure 1 F, Suppl. Figure 2 for activated T cells).

Nivolumab treatment of activated T cell cocultures has no effect on the expression of LAG-3, TIM-3 and TIGIT, while PD1 expression becomes undetectable

Expression of the immune checkpoint proteins PD1, LAG-3, TIM-3 and TIGIT was assessed by flow cytometry in activated $CD4^+$ and $CD8^+$ T cells before and after overnight coculture with the cHL cell line L-1236. The aim was to determine if the expression of other checkpoint proteins is altered after Nivolumab treatment. Activated T cells were used because relevant PD1 expression was only observed in activated T cells (Suppl. Figure 3). Both PD1 and LAG-3 expression was reduced in the cocultured $CD4^+$ and $CD8^+$ T cells in the presence of the IgG4 kappa isotype control antibody (Suppl. Figure 4). However, there was no difference in LAG-3 expression between Nivolumab and IgG4 kappa isotype treated cocultures. Using a PD-L1 knockout L-1236 cell line for the T cell cocultures, LAG-3 expression was significantly higher in the activated $CD4^+$ T cells compared to the activated $CD4^+$ T cells cocultured with the L-1236 control cell line (33.88 vs. 18.04% LAG-3 expression, Suppl. Figure 4D and E, $p<0.05$, Mann-Whitney-test), while all other checkpoint proteins were unchanged when using PD-L1 knockout L-1236 (Suppl. Figure 4).

Duration of T-cell contact with B-cells is not affected in normal lymphoid tissue after Nivolumab treatment

We then examined the motility of $CD4^+$ and $CD8^+$ T cells and $CD20^+$ B cells in native thick sections of native pharyngeal tonsil hyperplastic tissue, as we also observed PD-L1 expression in normal lymphoid tissue (Suppl. Figure 5). Time-lapse movies were taken immediately and after 3 and 5 hours. While the velocity of $CD4^+$ and $CD8^+$ T cells as well as $CD20^+$ B cells was almost unchanged at 3 and 5 h with and without Nivolumab, generally T cells were significantly faster when compared with B cells (means 3.77 and 3.40 µm/min for $CD4^+$ and $CD8^+$ T cells vs. 2.39 µm/min for B cells, $p<0.05$, Kruskal-Wallis-test with Dunn´s post-test for multiple comparisons). Similarly, there were no changes in track length or displacement for $CD4^+$, $CD8^+$ T cells or B cells after Nivolumab incubation (data not shown). After 5 hours of incubation with the IgG4 kappa isotype control antibody, the velocity of $CD4^+$ T cells was significantly higher compared to the untreated tissue slices ($p<0.05$, Kruskal-Wallis test, Figure 2A). This difference may be attributed to the limited sample size and the different areas of imaging, whether within or outside of follicles. In all other settings there was no effect on velocity of either Nivolumab nor IgG4 kappa isotype control antibody.

Cell-cell contacts in untreated tissue were shortest when $CD8^+$ cells were involved (CD8-CD20 mean 1.30 min, CD4-CD8 mean 1.65 min), whereas the duration of CD4-CD20 cell contacts under baseline conditions was longer (mean 3.72 min) and had a higher variance, reflecting the physiologic interaction of $CD4^+$ T cells and $CD20^+$ B cells in follicles and interfollicular areas. Overall, there was no clear effect of Nivolumab on cell contact duration in normal lymphoid tissue (Figure 2D, E and F). However, CD4-CD20 cell contacts were significantly longer after 5h of IgG4 kappa isotype control antibody incubation compared to the Nivolumab treated tissue slices (5.08 vs. 0.74 min, $p<0.01$, Kruskal-Wallis-test with Dunn's post-test for multiple testing, Figure 2D). This may be due to the limited number of samples and different areas of imaging.

HRS cells in cHL present enhanced cell-cell contacts with $CD4^+$ T cells after Nivolumab treatment

Next, we incubated thick slices of native tissue from cHL-affected lymph nodes with Nivolumab and took movies at baseline and after 3 and 5 h of Nivolumab incubation. All cases had PD-L1 positive HRS cells and bystander cells (Suppl. Figure 6). The velocity of $CD4^+$ T cells (2.87 - 4.94 µm/min), $CD8^+$ T cells (3.54 - 4.07 µm/min) and HRS cells (1.94-3.13 µm/min) was largely unchanged after 3 and 5h of Nivolumab incubation (Figure 3A). Similarly, track length and displacement were essentially unchanged in all cell types after 3 and 5h of Nivolumab incubation (data not shown). The number of cell-cell contacts between $CD4^+$ T cells and HRS cells was increased after 5h Nivolumab incubation (mean 1 contact/$CD4^+$ T cell/movie after 5h Nivolumab vs. mean 0.45 contact/$CD4^+$ T cell/movie at baseline, not significant, Figure 3B). No differences were seen in the number of cell contacts between $CD8^+$ T cells and HRS cells or between $CD4^+$ and $CD8^+$ T cells after Nivolumab incubation (Figure 3B). Regarding the duration of cell-cell contacts, a significant increase in the duration of cell-cell contacts between $CD4^+$ T cells and $CD30^+$ HRS cells was observed after 5h Nivolumab incubation (Figure 3C and E, after 5h Nivolumab mean 5.89 min vs. untreated mean 3.20 min, $p<0.05$, Kruskal-Wallis-test with Dunn´s post-test for multiple comparisons). At the same time, the duration of cell contacts between $CD8^+$ T cells and $CD30^+$ HRS cells was significantly increased after 5h of Nivolumab incubation (mean 3.73 min vs. mean 1.11 min in untreated setting, $p<0.05$, Kruskal-Wallis-test with Dunn´s post-test for multiple comparisons). There was no difference in the duration of cell contacts between $CD4^+$ and $CD8^+$ cells in the untreated vs. Nivolumab-treated groups (Figure 3C).

When only cHL cases with MHC I or II-positive HRS cells were considered (Suppl. Table 1, Suppl. Figure 7-9), the increase in cell-cell contact duration between $CD4^+$ T cells and HRS cells remained significant after 5h Nivolumab treatment. Differences in the duration of $CD8^+$ and HRS cell contacts were abolished, when only the subgroups of MHC I- or II-positive or -negative cases were considered.

When examining the duration of cell contact between $CD4^+$ and $CD8^+$ T cells and HRS cells after 5 h of Nivolumab incubation, it was found that there was a significantly longer duration of contact between $CD4^+$ T cells and HRS cells in MHC II-negative cHL cases compared to MHC II-positive cHL cases (mean of 8.31 min in MHC II-negative cases vs.

4.51 min in MHC I-positive cases, $p<0.05$, Mann-Whitney test, Figure 3D). The duration of contacts between $CD8^+$ T cells and HRS cells was also longer in cHL cases with MHC I-negative HRS cells (mean 5.15 min in MHC I-negative vs. 1.59 min in MHC I-positive cHL cases, not significant).

Figure 4 shows examples (from case 1) where long tracks with little displacement were seen in most cell types after 5h of Nivolumab treatment.

Discussion

This is the first study to demonstrate the dynamic effects of the anti-PD1 antibody Nivolumab on cell motility and cell-cell interactions of T cells, B cells and HRS cells in cHL using live cell imaging. Previously observed differences in the cell dynamics of immune cells[17] were confirmed in this study, with T cells moving significantly faster than B cells in hyperplastic lymphoid tissue.

As PD1 has been described to be expressed on non-malignant $CD4^+$, $CD8^+$ and $CD20^+$ cells[19], we would potentially expect to see effects in all these cell types as PD-L1 was almost ubiquitously expressed in the tissue (Suppl. Figures 5 and 6). However, overall cell motility was not altered after Nivolumab incubation in either microchannels, hyperplastic lymphoid tissue or primary cHL tissue, suggesting that there is no direct effect of Nivolumab on cell motility.

While the duration of cell-cell contacts between $CD4^+$ T cells and B cells in in hyperplastic lymphoid tissue was unchanged after Nivolumab treatment, resting $CD4^+$ T cells in microchannels showed significantly longer cell-cell contacts with HRS cells of the cHL cell line L-1236 as well as $CD4^+$ T cells with HRS cells in primary cHL tissue. Although the microchannel system is more artificial than imaging of primary tissue, this suggests that the situation in cHL is generally different from that in hyperplastic lymphoid tissue. While data from the literature suggests that the IFN-gamma pathway is active in both hyperplastic tonsillar tissue[20] and cHL[21, 22], there are several other differences between hyperplastic lymphoid tissue and cHL, such as the composition of the microenvironment, the frequent lack of MHC-I and -II expression in HRS cells, the tumour mutation burden, which has been observed to be on average 3.57/Mb in cHL nodular sclerosing type[23], as well as differences in chemokine secretion in the

neoplastic HRS cells of cHL. In this regard, tumour mutational burden, microsatellite instability, expression of tumour neoantigens, epigenetic silencing, expression of chemokines and receptors such as CCR5, CXCL9 and CXLC13, have been described to be associated with response to checkpoint inhibitor therapy.[24-26] These findings may explain the divergent observation of cell-cell interaction after Nivolumab treatment in our study and also the large variance between samples, as each patient or tissue has individual factors that influence the efficacy of checkpoint inhibition. HRS cells from cHL strongly secrete various chemokines such as CXCL9, CCL5, CCL17 and CCL22 and thus attract both $CD4^+$ and $CD8^+$ T cells.[21,27-29] While an inferior outcome after checkpoint inhibition was observed in patients with loss of MHC I protein expression in HRS cells of cHL[30], we found rather prolonged cell contacts of $CD8^+$ T cells and HRS cells in cHL with MHC I loss (not significant). Similarly, the duration of cell-cell contacts between $CD4^+$ T cells and HRS cells was significantly longer when MHC II expression was absent in HRS cells. This suggests that the effects of Nivolumab are, to some extent, independent of MHC expression.

The in vitro cHL model can be extended in the future to study T cell activation by visualizing intracellular Ca^{2+} signalling and measuring T cell cytotoxicity. The importance of $CD4^+$ T cells in mediating the effects of Nivolumab has previously been demonstrated in several studies, including the significant expansion of the $CD4^+$ T cell receptor repertoire in the peripheral blood of patients responding to Nivolumab treatment.[31] In addition, lymph node biopsies taken one week after start of Nivolumab therapy showed little change in the frequency of $CD4^+$ and $CD8^+$ T cells in the cHL microenvironment, despite the frequent disappearance of neoplastic $CD30^+$ HRS cells.[32]

Another study found that clonally expanded T cells in untreated cHL lymph nodes were rare, were exclusively $CD8^+$, had a non-naïve immune phenotype and only a minority of them expressed classical immune checkpoint molecules.[33] Another study showed that MHC II expression on the HRS cells was predictive of response to Nivolumab treatment whereas no such correlation was observed for MHC I expression on HRS cells.[18] One hypothesis for how Nivolumab might work is that subsets of rosetting $CD4^+$ T cells, which contribute to the growth support of the HRS cells[34], move away from the HRS

cells, resulting in the removal of growth support. Immunological synapses were observed between HRS cells and rosetting T cells in this regard.[35]

The phenotype of $CD4^+$ T cells with regard to LAG-3, TIM-3 or TIGIT expression did not change after Nivolumab incubation in our *in vitro* coculture model of cHL. On the one hand, this model has the limitation that $CD4^+$ and $CD8^+$ T cells were purified from peripheral blood and did not undergo long-term coculture with HRS cells. On the other hand, the phenotype of $CD8^+$ T cells after checkpoint inhibition in a melanoma patient, studied on single cell level in the literature, also did not change with respect to LAG-3, TIM-3 or TIGIT expression.[36] Co-inhibition of other checkpoint proteins may therefore be an additional therapeutic option.

In general, most studies, including ours, have focussed on the effects of Nivolumab on the activity of $CD4^+$ or $CD8^+$ T cells. Effects on other cell types such as histiocytes, macrophages and NK cells have not been studied in cHL and may provide explanations for the remaining unanswered questions about the effect of Nivolumab. In a mouse model, it was observed that anti-PD1 antibody can be captured from $CD8^+$ T cells by macrophages leading to resistance to checkpoint inhibition.[37]

In conclusion, Nivolumab altered cell-cell interactions between $CD4^+$ T cells and $CD30^+$ HRS cells in cHL. The significant prolongation of cell-cell contacts between $CD4^+$ T cells and HRS cells may be one component of the successful mode of action of Nivolumab in cHL. In this study, the effects of Nivolumab were found to be independent of the expression of MHC I or II on HRS cells. Future studies, analysing the correlation between Nivolumab-induced changes in motility, cell-cell contacts and outcome after therapy are warranted.

References

1. Balzano C, Buonavista N, Rouvier E, et al. CTLA-4 and CD28: similar proteins, neighbouring genes. Int J Cancer Suppl. 1992;7:28-32.
2. Nishimura H, Nose M, Hiai H, et al. Development of lupus-like autoimmune diseases by disruption of the PD-1 gene encoding an ITIM motif-carrying immunoreceptor. Immunity. 1999;11(2):141-151.
3. Okazaki T, Honjo T. PD-1 and PD-1 ligands: from discovery to clinical application. Int Immunol. 2007;19(7):813-824.
4. Ott PA, Bang YJ, Piha-Paul SA, et al. T-Cell-Inflamed Gene-Expression Profile, Programmed Death Ligand 1 Expression, and Tumor Mutational Burden Predict Efficacy in Patients Treated With Pembrolizumab Across 20 Cancers: KEYNOTE-028. J Clin Oncol. 2019;37(4):318-327.
5. Chen R, Zinzani PL, Fanale MA, et al. Phase II Study of the Efficacy and Safety of Pembrolizumab for Relapsed/Refractory Classic Hodgkin Lymphoma. J Clin Oncol. 2017;35(19):2125-2132.
6. Armand P, Engert A, Younes A, et al. Nivolumab for Relapsed/Refractory Classic Hodgkin Lymphoma After Failure of Autologous Hematopoietic Cell Transplantation: Extended Follow-Up of the Multicohort Single-Arm Phase II CheckMate 205 Trial. J Clin Oncol. 2018;36(14):1428-1439.
7. Ansell SM, Lesokhin AM, Borrello I, et al. PD-1 blockade with nivolumab in relapsed or refractory Hodgkin's lymphoma. N Engl J Med. 2015;372(4):311-319.
8. Brockelmann PJ, Goergen H, Keller U, et al. Efficacy of Nivolumab and AVD in Early-Stage Unfavorable Classic Hodgkin Lymphoma: The Randomized Phase 2 German Hodgkin Study Group NIVAHL Trial. JAMA Oncol. 2020;6(6):872-880
9. Brockelmann PJ, Buhnen I, Meissner J, et al. Nivolumab and Doxorubicin, Vinblastine, and Dacarbazine in Early-Stage Unfavorable Hodgkin Lymphoma: Final Analysis of the Randomized German Hodgkin Study Group Phase II NIVAHL Trial. J Clin Oncol. 2023;41(6):1193-1199.
10. Ramchandren R, Domingo-Domenech E, Rueda A, et al. Nivolumab for Newly Diagnosed Advanced-Stage Classic Hodgkin Lymphoma: Safety and Efficacy in the Phase II CheckMate 205 Study. J Clin Oncol. 2019;37(23):1997-2007.
11. Allen PB, Savas H, Evens AM, et al. Pembrolizumab followed by AVD in untreated early unfavorable and advanced-stage classical Hodgkin lymphoma. Blood. 2021;137(10):1318-1326.
12. Joyce JA, Fearon DT. T cell exclusion, immune privilege, and the tumor microenvironment. Science. 2015;348(6230):74-80.
13. Fife BT, Pauken KE, Eagar TN, et al. Interactions between PD-1 and PD-L1 promote tolerance by blocking the TCR-induced stop signal. Nat Immunol. 2009;10(11):1185-1192.
14. Honda T, Egen JG, Lammermann T, et al. Tuning of antigen sensitivity by T cell receptor-dependent negative feedback controls T cell effector function in inflamed tissues. Immunity. 2014;40(2):235-247.
15. Lau D, Garcon F, Chandra A, et al. Intravital Imaging of Adoptive T-Cell Morphology, Mobility and Trafficking Following Immune Checkpoint Inhibition in a Mouse Melanoma Model. Front Immunol. 2020;11:1514.

16. Goncharova O, Flinner N, Bein J, et al. Migration Properties Distinguish Tumor Cells of Classical Hodgkin Lymphoma from Anaplastic Large Cell Lymphoma Cells. Cancers (Basel). 2019;11(10):1484.
17. Hartmann S, Scharf S, Steiner Y, et al. Landscape of 4D Cell Interaction in Hodgkin and Non-Hodgkin Lymphomas. Cancers (Basel). 2021;13(20):5208.
18. Roemer MGM, Redd RA, Cader FZ, et al. Major Histocompatibility Complex Class II and Programmed Death Ligand 1 Expression Predict Outcome After Programmed Death 1 Blockade in Classic Hodgkin Lymphoma. J Clin Oncol. 2018;36(10):942-950.
19. Sharpe AH, Pauken KE. The diverse functions of the PD1 inhibitory pathway. Nat Rev Immunol. 2018;18(3):153-167.
20. Quiding M, Granstrom G, Nordstrom I, et al. High frequency of spontaneous interferon-gamma-producing cells in human tonsils: role of local accessory cells and soluble factors. Clin Exp Immunol. 1993;91(1):157-163.
21. Vassilakopoulos TP, Levidou G, Milionis V, et al. Thioredoxin-1, chemokine (C-X-C motif) ligand-9 and interferon-gamma expression in the neoplastic cells and macrophages of Hodgkin lymphoma: clinicopathologic correlations and potential prognostic implications. Leuk Lymphoma. 2017;58(9):1-13.
22. Gholiha AR, Hollander P, Lof L, et al. Immune-Proteome Profiling in Classical Hodgkin Lymphoma Tumor Diagnostic Tissue. Cancers (Basel). 2021;14(1):9.
23. Tiacci E, Ladewig E, Schiavoni G, et al. Pervasive mutations of JAK-STAT pathway genes in classical Hodgkin lymphoma. Blood. 2018;131(22):2454-2465.
24. Litchfield K, Reading JL, Puttick C, et al. Meta-analysis of tumor- and T cell-intrinsic mechanisms of sensitization to checkpoint inhibition. Cell. 2021;184(3):596-614.
25. Makuku R, Khalili N, Razi S, et al. Current and Future Perspectives of PD-1/PDL-1 Blockade in Cancer Immunotherapy. J Immunol Res. 2021;2021:6661406.
26. Peng D, Kryczek I, Nagarsheth N, et al. Epigenetic silencing of TH1-type chemokines shapes tumour immunity and immunotherapy. Nature. 2015;527(7577):249-253.
27. van den Berg A, Visser L, Poppema S. High expression of the CC chemokine TARC in Reed-Sternberg cells. A possible explanation for the characteristic T-cell infiltration Hodgkin's lymphoma. Am J Pathol. 1999;154(6):1685-1691.
28. Hartmann S, Jakobus C, Rengstl B, et al. Spindle-shaped CD163+ rosetting macrophages replace CD4+ T-cells in HIV-related classical Hodgkin lymphoma. Mod Pathol. 2013;26(5):648-657.
29. Döring C, Hansmann ML, Agostinelli C, et al. A novel immunohistochemical classifier to distinguish Hodgkin lymphoma from ALK anaplastic large cell lymphoma. Mod Pathol. 2014;27(10):1345-1354.
30. Roemer MG, Advani RH, Redd RA, et al. Classical Hodgkin Lymphoma with Reduced beta2M/MHC Class I Expression Is Associated with Inferior Outcome Independent of 9p24.1 Status. Cancer Immunol Res. 2016;4(11):910-916.
31. Cader FZ, Hu X, Goh WL, et al. A peripheral immune signature of responsiveness to PD-1 blockade in patients with classical Hodgkin lymphoma. Nat Med. 2020;26(9):1468-1479.
32. Reinke S, Brockelmann PJ, Iaccarino I, et al. Tumor and microenvironment response but no cytotoxic T-cell activation in classic Hodgkin lymphoma treated with anti-PD1. Blood. 2020;136(25):2851-2863.

33. Ballhausen A, Ben Hamza A, Welters C, et al. Immune phenotypes and checkpoint molecule expression of clonally expanded lymph node-infiltrating T cells in classical Hodgkin lymphoma. Cancer Immunol Immunother. 2023;72(2):515-521.
34. Weniger MA, Kuppers R. Molecular biology of Hodgkin lymphoma. Leukemia. 2021;35(4):968-981.
35. Veldman J, Visser L, Huberts-Kregel M, et al. Rosetting T cells in Hodgkin lymphoma are activated by immunological synapse components HLA class II and CD58. Blood. 2020;136(21):2437-2441.
36. Khojandi N, Connelly L, Piening A, et al. Single-cell analysis of peripheral CD8(+) T cell responses in patients receiving checkpoint blockade immunotherapy for cancer. Cancer Immunol Immunother. 2023;72(2):397-408.
37. Arlauckas SP, Garris CS, Kohler RH, et al. In vivo imaging reveals a tumor-associated macrophage-mediated resistance pathway in anti-PD-1 therapy. Sci Transl Med. 2017;9(389):eaal3604.

Figure Legend

Figure 1. Effects of Nivolumab on T cell motility in microchannels in the presence of Hodgkin-Reed-Sternberg (HRS) cells

A. Schematic overview of experimental setup with 4x10 µm microchannels connecting two reservoirs containing either $CD4^+$ or $CD8^+$ T cells (left side) and classic Hodgkin lymphoma (cHL) cell lines (right side).
B. PD-L1 expression in the classic Hodgkin lymphoma cell lines L-428 and L-1236 (black) compared with isotype control (grey)
C. Velocity of resting $CD4^+$ and $CD8^+$ T cells in microchannels with and without Nivolumab or with IgG4 kappa isotype control in presence of classic Hodgkin lymphoma cell lines
D. Velocity of activated $CD4^+$ and $CD8^+$ T cells in microchannels with and without Nivolumab or with IgG4 kappa isotype control in presence of classic Hodgkin lymphoma cell lines
E. Duration of cell-cell contacts between Hodgkin-Reed-Sternberg cells of cell line L-1236 and resting $CD4^+$ or $CD8^+$ T cells with or without Nivolumab or with IgG4 kappa isotype control
F. Duration of cell-cell contacts between Hodgkin-Reed-Sternberg cells of cell line L-428 and resting $CD4^+$ or $CD8^+$ T cells with or without Nivolumab or with IgG4 kappa isotype control
G. Example of several short duration contacts between a resting $CD4^+$ T cell and a Hodgkin-Reed-Sternberg cell without Nivolumab (Hodgkin-Reed-Sternberg cell green, $CD4^+$ T cell red)
H. Example of a long duration contact between a resting $CD4^+$ T cell and a Hodgkin-Reed-Sternberg cell with Nivolumab (Hodgkin-Reed-Sternberg cell green, $CD4^+$ T cell red)

Figure 2. Cell velocity and duration of cell-cell contacts in hyperplastic lymphoid tissue

Each dot represents the mean of a movie. Typically, three movies per condition were obtained.

A. Velocity of $CD4^+$ T cells in hyperplastic lymphoid tissue (from thirteen donors) with and without Nivolumab or IgG4 kappa isotype control antibody; * $p<0.05$, Kruskal-Wallis-test with Dunn´s post-test for multiple testing
B. Velocity of $CD8^+$ T cells in hyperplastic lymphoid tissue (from thirteen donors) with and without Nivolumab or IgG4 kappa isotype control antibody
C. Velocity of $CD20^+$ B cells in hyperplastic lymphoid tissue (from thirteen donors) with and without Nivolumab or IgG4 kappa isotype control antibody
D. Duration of cell-cell contacts between $CD4^+$ T cells and $CD20^+$ B cells in hyperplastic lymphoid tissue (from thirteen donors) with and without Nivolumab or IgG4 kappa isotype control antibody; * $p<0.05$, Kruskal-Wallis-test with Dunn´s post-test for multiple testing

E. Duration of cell-cell contacts between $CD8^+$ T cells and $CD20^+$ B cells in hyperplastic lymphoid tissue (from thirteen donors) with and without Nivolumab or IgG4 kappa isotype control antibody
F. Examples for a short cell contact (left) between a $CD8^+$ T cell (arrow head) and a $CD20^+$ B cell (arrow, green cell) and longer duration cell contact (right) between a $CD8^+$ T cell (arrow head, red cell) and a $CD20^+$ B cell (arrow, green cell);
$CD8^+$ T cells labelled in red, $CD20^+$ B cell labelled in green.

Figure 3. Nivolumab incubation extends cell-cell contacts between $CD4^+$ T cells and Hodgkin-Reed-Sternberg (HRS) cells in classic Hodgkin lymphoma.
The study analysed six cases of classic Hodgkin lymphoma, including five cases in both untreated and Nivolumab-treated conditions, and one case in untreated condition only. Each dot represents the mean of a movie. Typically, three movies per condition were obtained.

A. Velocity of $CD4^+$ and $CD8^+$ T cells as well as $CD30^+$ Hodgkin-Reed-Sternberg cells in classic Hodgkin lymphoma in untreated condition (0h) and after incubation with Nivolumab for 3 or 5 hrs
B. Number of cell-cell contacts between individual $CD4^+$ T cells/movie and $CD30^+$ Hodgkin-Reed-Sternberg cells, individual $CD8^+$ T cells/movie and $CD30^+$ Hodgkin-Reed-Sternberg cells as well as $CD4^+$ and $CD8^+$ T cells in classic Hodgkin lymphoma in untreated condition (0h) and after incubation with Nivolumab (3h and 5h)
C. Duration of cell-cell contacts between $CD4^+$ T cells and $CD30^+$ Hodgkin-Reed-Sternberg cells, $CD8^+$ T cells and $CD30^+$ Hodgkin-Reed-Sternberg cells as well as $CD4^+$ and $CD8^+$ T cells in classic Hodgkin lymphoma in untreated condition (0h) and after incubation with Nivolumab (3h and 5h). * $p<0.05$, Kruskal-Wallis-test with Dunn´s post-test for multiple testing
D. Duration of cell-cell contacts between $CD4^+$ T cells and $CD30^+$ Hodgkin-Reed-Sternberg cells as well as $CD8^+$ T cells and $CD30^+$ Hodgkin-Reed-Sternberg cells after 5h Nivolumab incubation. Cases were stratified based on MHC I and II expression in the Hodgkin-Reed-Sternberg cells. * $p<0.05$, Kruskal-Wallis-test with Dunn´s post-test for multiple testing
E. Examples for a short cell contact (left) between three $CD4^+$ T cells (arrow heads) and a $CD30^+$ Hodgkin-Reed-Sternberg cells (#) in untreated condition and long duration cell contact (right) between a $CD4^+$ T cell (arrow head) and a $CD30^+$ Hodgkin-Reed-Sternberg cell (#); $CD4^+$ T cells labelled in pink, $CD30^+$ Hodgkin-Reed-Sternberg cell labelled in green.

Figure 4. Cell tracks in classic Hodgkin lymphoma without and with Nivolumab
Top row shows images (merged, CD4 pink, CD8 red, CD30 green) and the respective tracks of the cells in a 15 min movie of untreated classic Hodgkin lymphoma tissue.

Bottom row shows images (merged, CD4 pink, CD8 red, CD30 green) and the respective tracks of the cells in a 15 min movie of classic Hodgkin lymphoma tissue from the same case after incubation with Nivolumab for 5 h. Speed scale bars in µm/sec.

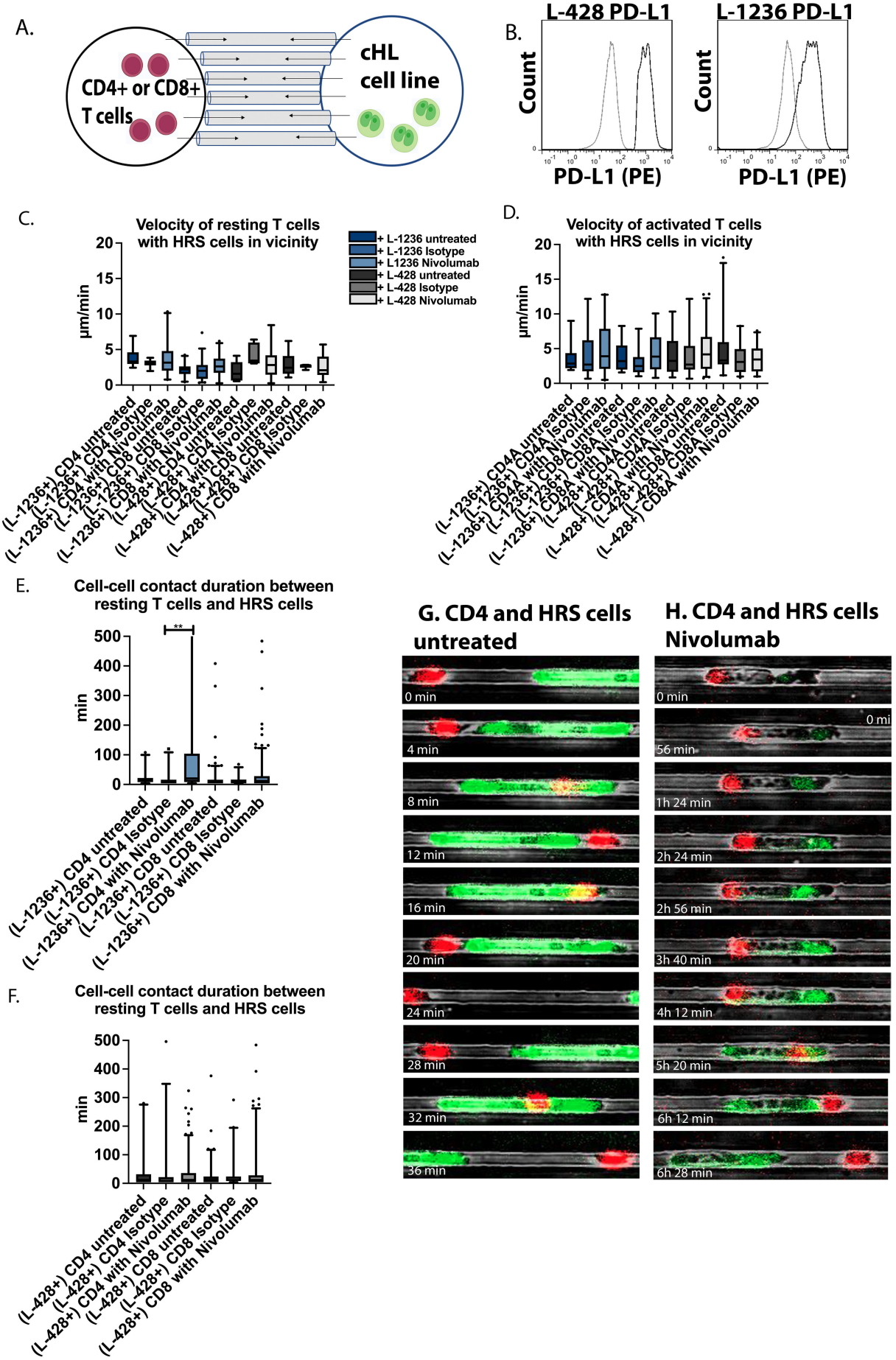
A.
CD4+ or CD8+
T cells
cHL
cell line
B.
L-428 PD-L1
L-1236 PD-L1
Count
PD-L1 (PE)
C.
Velocity of resting T cells
with HRS cells in vicinity
µm/min
+ L-1236 untreated
+ L-1236 Isotype
+ L1236 Nivolumab
+ L-428 untreated
+ L-428 Isotype
+ L-428 Nivolumab
(L-1236+) CD4 untreated
(L-1236+) CD4 Isotype
(L-1236+) CD4 with Nivolumab
(L-1236+) CD8 untreated
(L-1236+) CD8 Isotype
(L-1236+) CD8 with Nivolumab
(L-428+) CD4 untreated
(L-428+) CD4 Isotype
(L-428+) CD4 with Nivolumab
(L-428+) CD8 untreated
(L-428+) CD8 Isotype
(L-428+) CD8 with Nivolumab
D.
Velocity of activated T cells
with HRS cells in vicinity
µm/min
(L-1236+) CD4A untreated
(L-1236+) CD4A Isotype
(L-1236+) CD4A with Nivolumab
(L-1236+) CD8A untreated
(L-1236+) CD8A Isotype
(L-1236+) CD8A with Nivolumab
(L-428+) CD4A untreated
(L-428+) CD4A Isotype
(L-428+) CD4A with Nivolumab
(L-428+) CD8A untreated
(L-428+) CD8A Isotype
(L-428+) CD8A with Nivolumab
E.
Cell-cell contact duration between
resting T cells and HRS cells
min
**
(L-1236+) CD4 untreated
(L-1236+) CD4 Isotype
(L-1236+) CD4 with Nivolumab
(L-1236+) CD8 untreated
(L-1236+) CD8 Isotype
(L-1236+) CD8 with Nivolumab
F.
Cell-cell contact duration between
resting T cells and HRS cells
min
(L-428+) CD4 untreated
(L-428+) CD4 Isotype
(L-428+) CD4 with Nivolumab
(L-428+) CD8 untreated
(L-428+) CD8 Isotype
(L-428+) CD8 with Nivolumab
G. CD4 and HRS cells
untreated
0 min
4 min
8 min
12 min
16 min
20 min
24 min
28 min
32 min
36 min
H. CD4 and HRS cells
Nivolumab
0 min
56 min
1h 24 min
2h 24 min
2h 56 min
3h 40 min
4h 12 min
5h 20 min
6h 12 min
6h 28 min

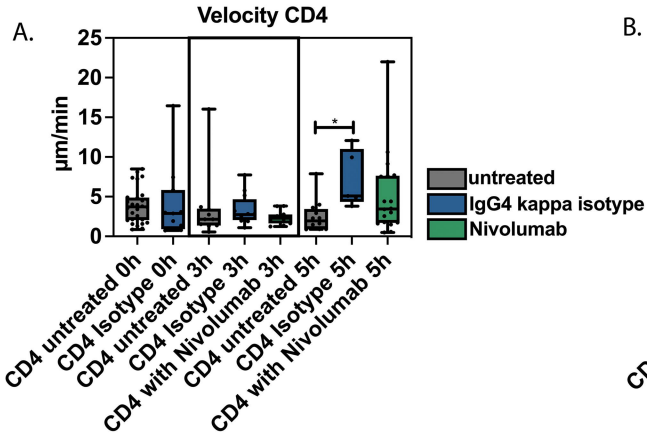
A.
Velocity CD4
µm/min
25
20
15
10
5
0
*
untreated
IgG4 kappa isotype
Nivolumab
CD4 untreated 0h
CD4 Isotype 0h
CD4 untreated 3h
CD4 Isotype 3h
CD4 with Nivolumab 3h
CD4 untreated 5h
CD4 Isotype 5h
CD4 with Nivolumab 5h

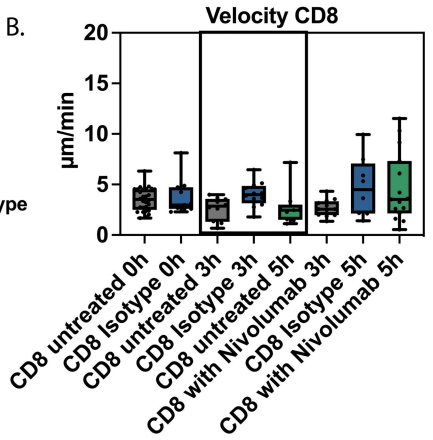
B.
Velocity CD8
µm/min
20
15
10
5
0
CD8 untreated 0h
CD8 Isotype 0h
CD8 untreated 3h
CD8 Isotype 3h
CD8 with Nivolumab 3h
CD8 untreated 5h
CD8 Isotype 5h
CD8 with Nivolumab 5h

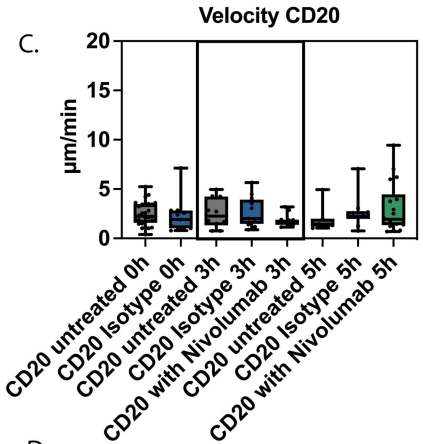
C.
Velocity CD20
µm/min
20
15
10
5
0
CD20 untreated 0h
CD20 Isotype 0h
CD20 untreated 3h
CD20 Isotype 3h
CD20 with Nivolumab 3h
CD20 untreated 5h
CD20 Isotype 5h
CD20 with Nivolumab 5h

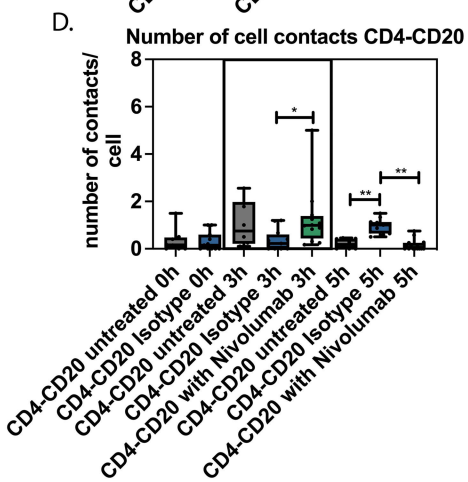
D.
Number of cell contacts CD4-CD20
number of contacts/ cell
8
6
4
2
0
*
**
**
CD4-CD20 untreated 0h
CD4-CD20 Isotype 0h
CD4-CD20 untreated 3h
CD4-CD20 Isotype 3h
CD4-CD20 with Nivolumab 3h
CD4-CD20 untreated 5h
CD4-CD20 Isotype 5h
CD4-CD20 with Nivolumab 5h

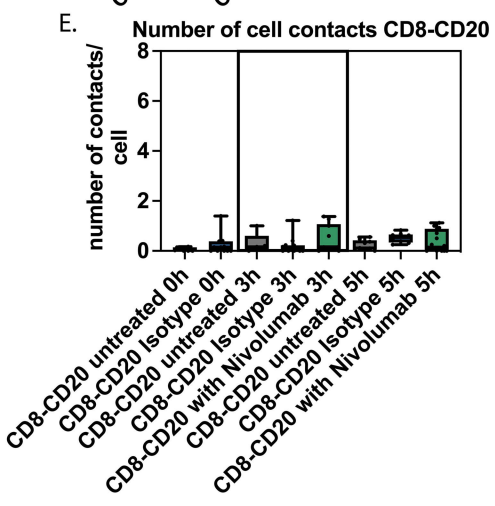
E.
Number of cell contacts CD8-CD20
number of contacts/ cell
8
6
4
2
0
CD8-CD20 untreated 0h
CD8-CD20 Isotype 0h
CD8-CD20 untreated 3h
CD8-CD20 Isotype 3h
CD8-CD20 with Nivolumab 3h
CD8-CD20 untreated 5h
CD8-CD20 Isotype 5h
CD8-CD20 with Nivolumab 5h

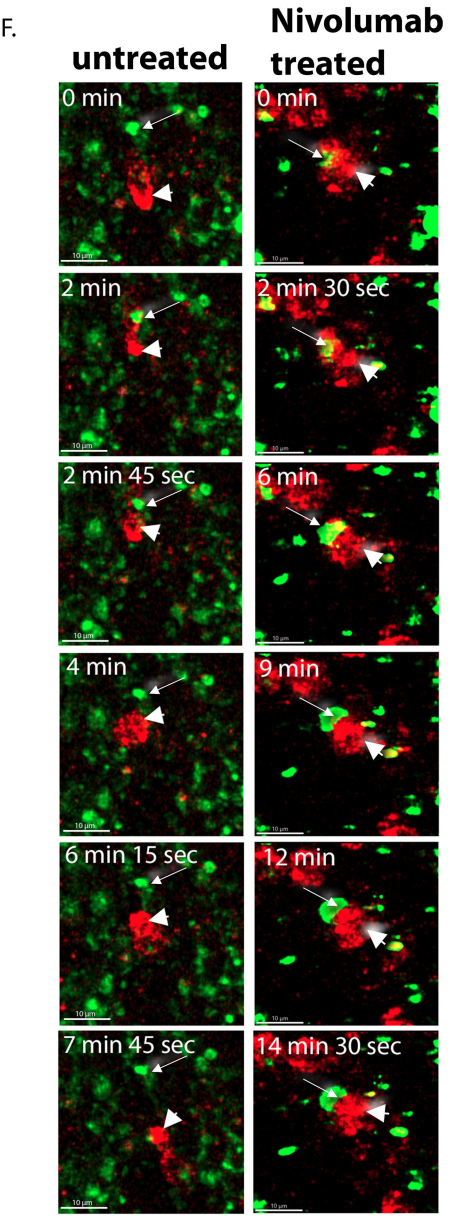
F.
untreated
Nivolumab treated
0 min
0 min
2 min
2 min 30 sec
2 min 45 sec
6 min
4 min
9 min
6 min 15 sec
12 min
7 min 45 sec
14 min 30 sec

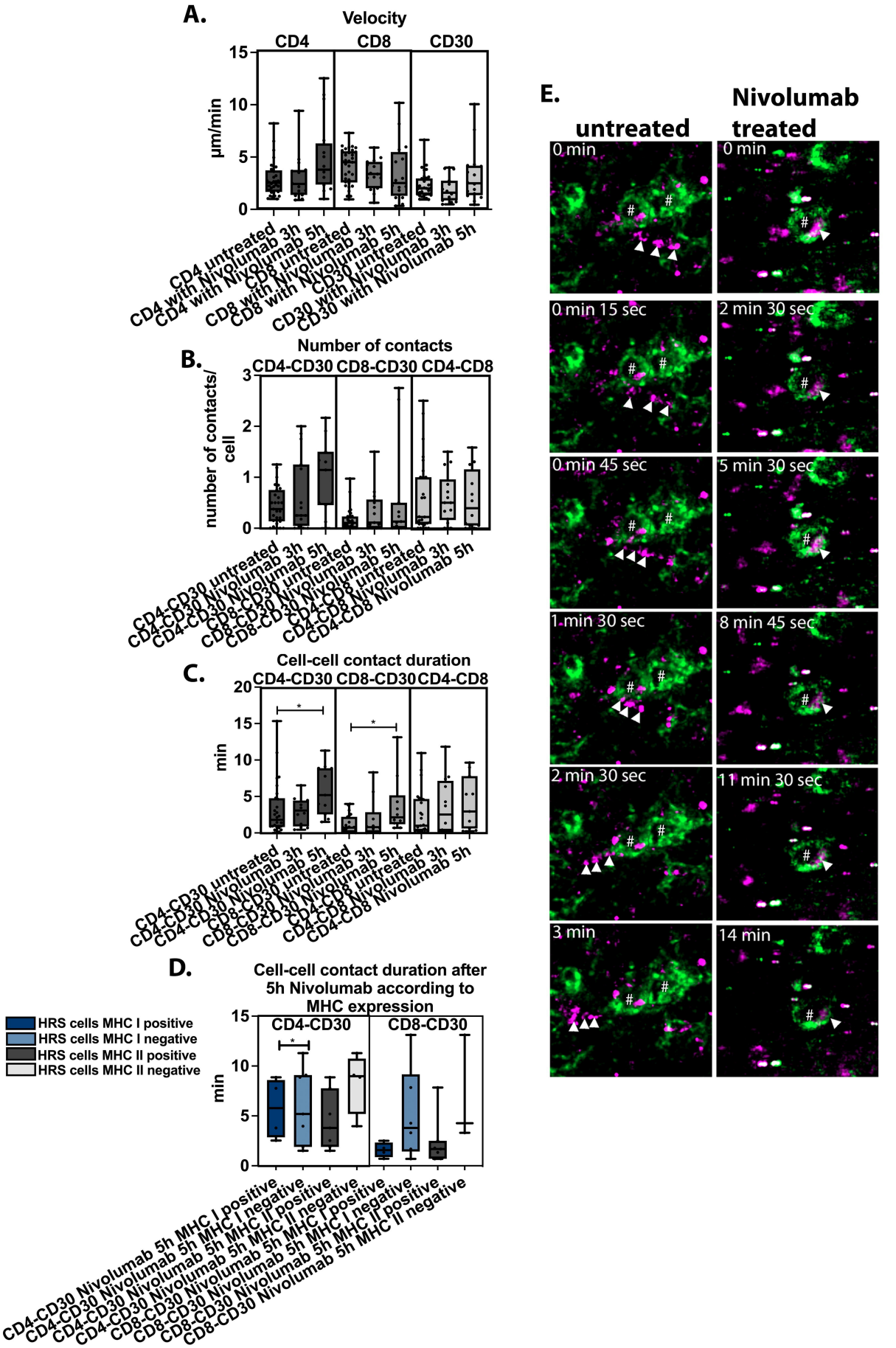
A.
Velocity
CD4
CD8
CD30
µm/min
15
10
5
0
CD4 untreated
CD4 with Nivolumab 3h
CD4 with Nivolumab 5h
CD8 untreated
CD8 with Nivolumab 3h
CD8 with Nivolumab 5h
CD30 untreated
CD30 with Nivolumab 3h
CD30 with Nivolumab 5h
B.
Number of contacts
CD4-CD30
CD8-CD30
CD4-CD8
number of contacts/ cell
3
2
1
0
CD4-CD30 untreated
CD4-CD30 Nivolumab 3h
CD4-CD30 Nivolumab 5h
CD8-CD30 untreated
CD8-CD30 Nivolumab 3h
CD8-CD30 Nivolumab 5h
CD4-CD8 untreated
CD4-CD8 Nivolumab 3h
CD4-CD8 Nivolumab 5h
C.
Cell-cell contact duration
CD4-CD30
CD8-CD30
CD4-CD8
min
20
15
10
5
0
*
*
CD4-CD30 untreated
CD4-CD30 Nivolumab 3h
CD4-CD30 Nivolumab 5h
CD8-CD30 untreated
CD8-CD30 Nivolumab 3h
CD8-CD30 Nivolumab 5h
CD4-CD8 untreated
CD4-CD8 Nivolumab 3h
CD4-CD8 Nivolumab 5h
D.
Cell-cell contact duration after 5h Nivolumab according to MHC expression
HRS cells MHC I positive
HRS cells MHC I negative
HRS cells MHC II positive
HRS cells MHC II negative
CD4-CD30
CD8-CD30
min
15
10
5
0
*
CD4-CD30 Nivolumab 5h MHC I positive
CD4-CD30 Nivolumab 5h MHC I negative
CD4-CD30 Nivolumab 5h MHC II positive
CD4-CD30 Nivolumab 5h MHC II negative
CD8-CD30 Nivolumab 5h MHC I positive
CD8-CD30 Nivolumab 5h MHC I negative
CD8-CD30 Nivolumab 5h MHC II positive
CD8-CD30 Nivolumab 5h MHC II negative
E.
untreated
Nivolumab treated
0 min
0 min
0 min 15 sec
2 min 30 sec
0 min 45 sec
5 min 30 sec
1 min 30 sec
8 min 45 sec
2 min 30 sec
11 min 30 sec
3 min
14 min
#

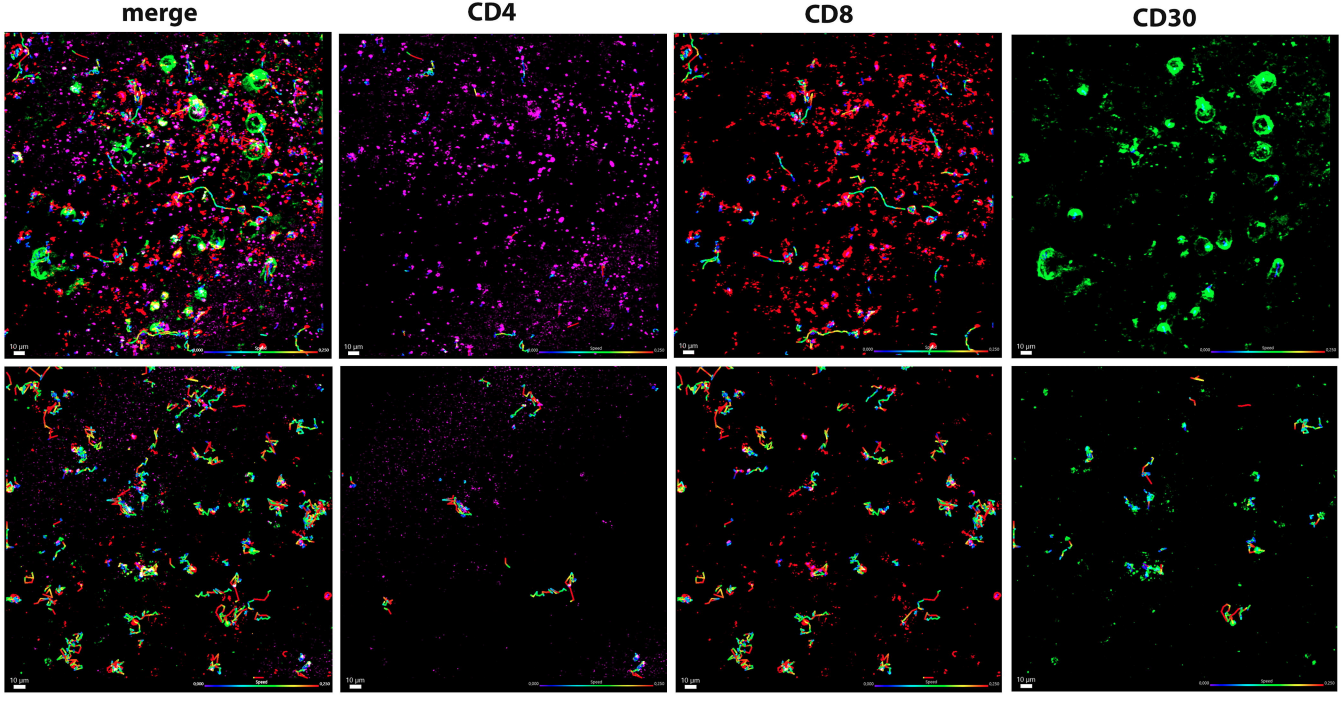
merge
CD4
CD8
CD30
untreated
Nivolumab

Supplementary Figures and Methods

Supplementary Figures

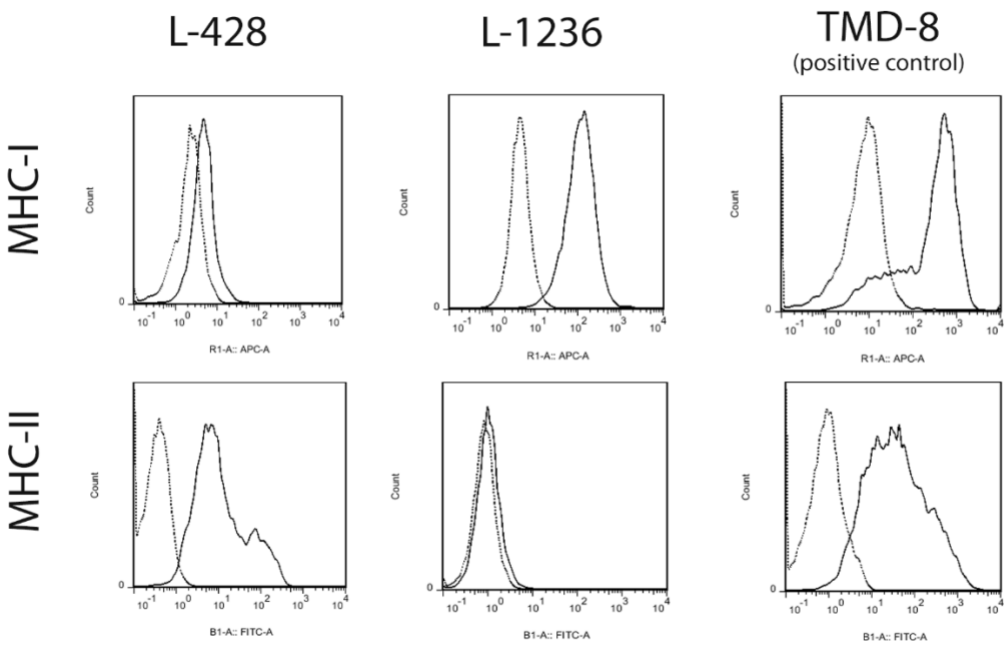

Suppl. Figure 1. MHC-I and –II expression in classic Hodgkin lymphoma cell lines L-428 and L-1236
Upper row: MHC-I expression as determined by FACS (bold line) versus isotype control (dotted line). The diffuse large B-cell lymphoma cell line TMD-8 was used as positive control.
Bottom row: MHC-II expression as determined by FACS (bold line) versus isotype control (dotted line). The diffuse large B-cell lymphoma cell line TMD-8 was used as positive control.

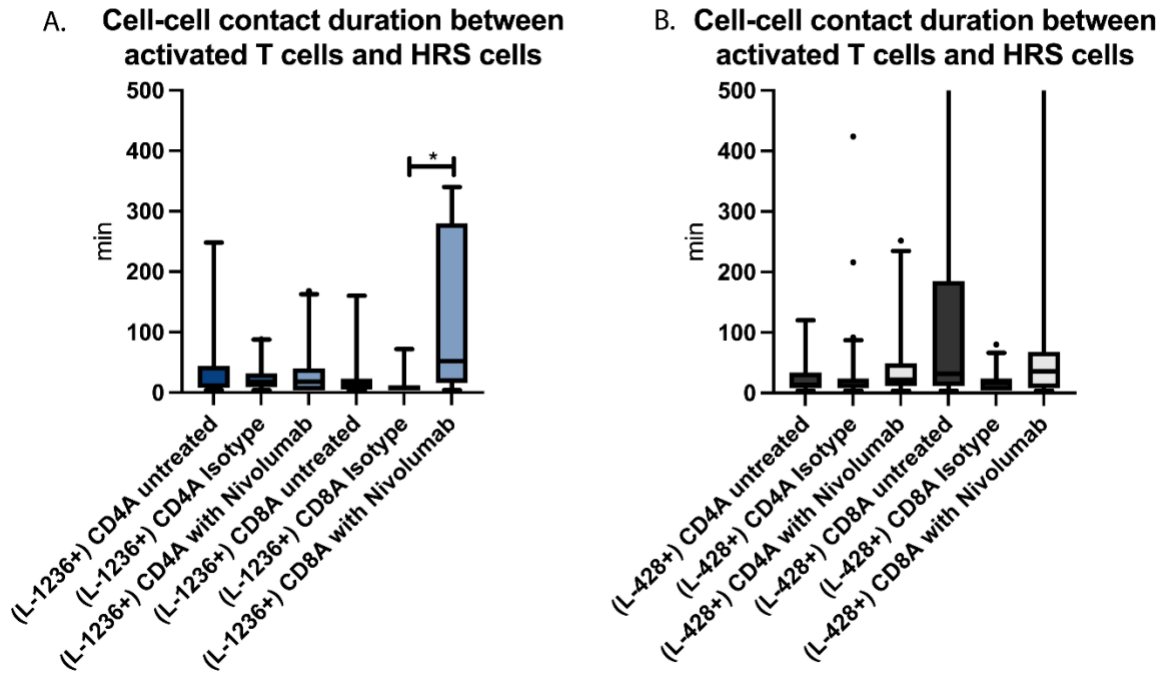

Suppl. Figure 2. Duration of cell-cell contacts between Hodgkin-Reed-Sternberg (HRS) cells and activated T cells

A. Duration of cell-cell contacts between HRS cells of cell line L-1236 and activated $CD4^+$ or $CD8^+$ T cells with or without Nivolumab or with IgG4 kappa isotype control
   * $p<0.05$, Kruskal-Wallis test
B. Duration of cell-cell contacts between HRS cells of cell line L-428 and activated $CD4^+$ or $CD8^+$ T cells with or without Nivolumab or with IgG4 kappa isotype control

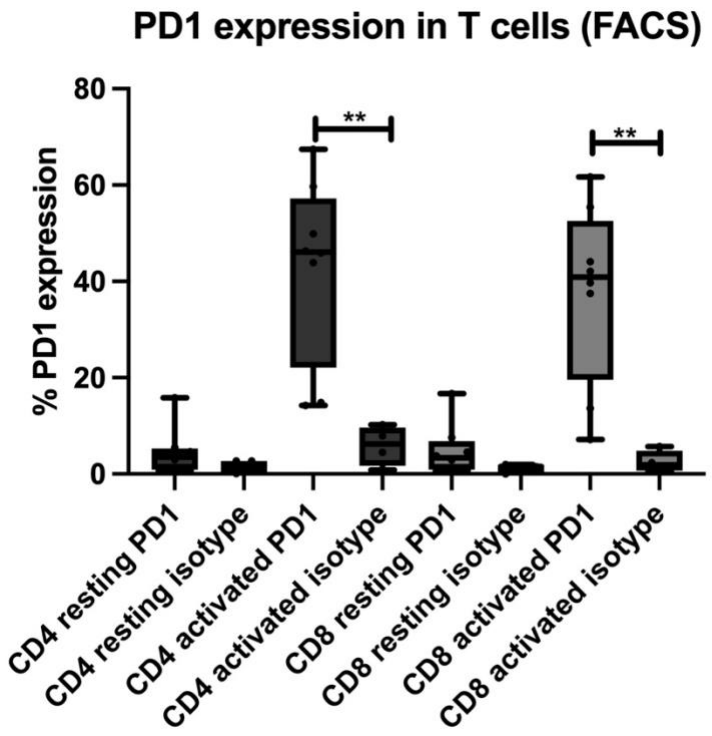

Suppl. Figure 3. PD1 expression by flow cytometry in T cells
PD1 expression by flow cytometry in resting and activated $CD4^+$ and $CD8^+$ T cells used in microchannel experiments, compared to isotype control

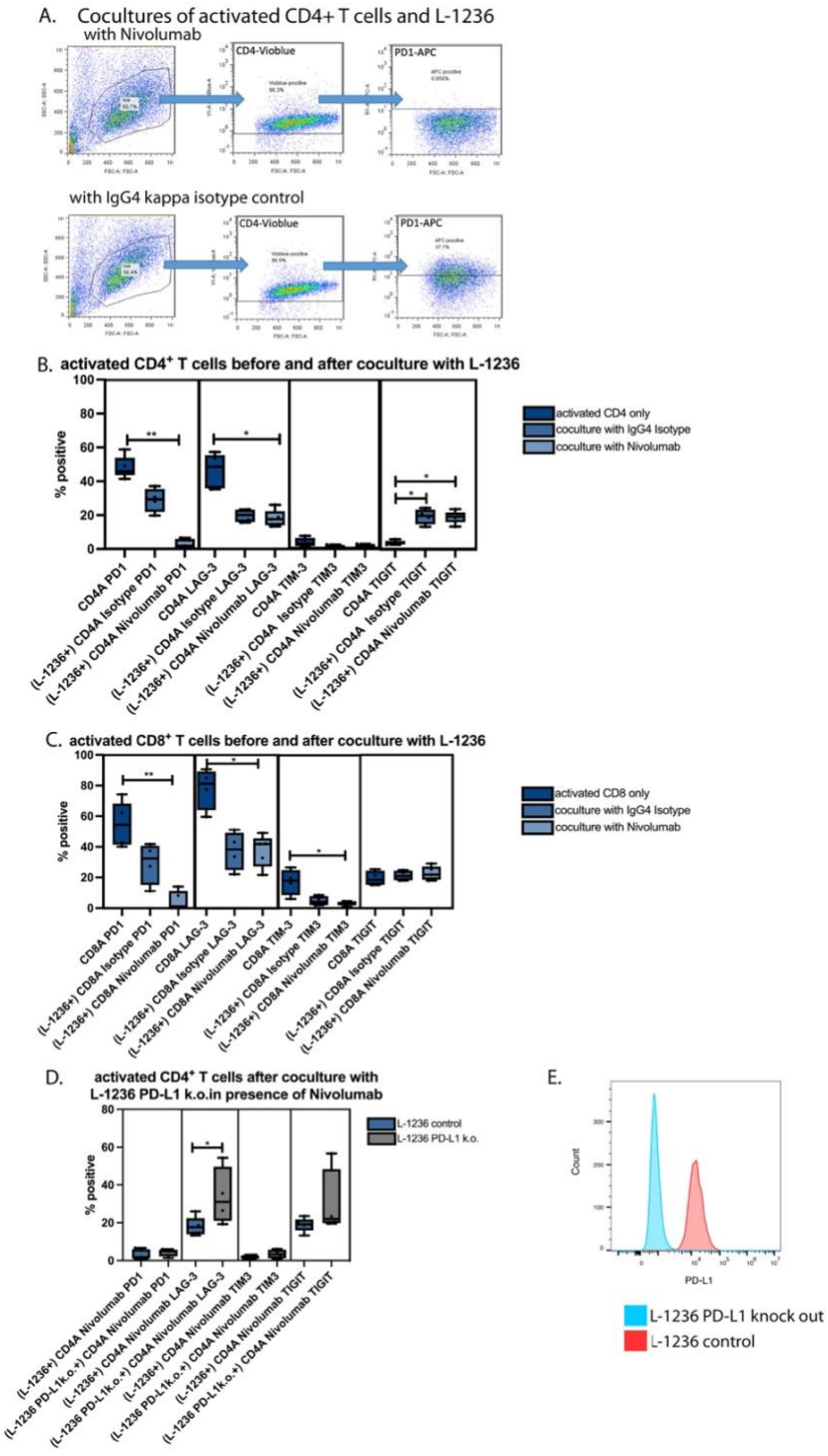

Suppl. Figure 4. Expression of the immune checkpoint proteins PD1, LAG-3, TIM-3 and TIGIT in an *in vitro* coculture model of classic Hodgkin lymphoma

A. Examples of a 20:1 overnight coculture of activated $CD4^+$ T cells and HRS cells from the L-1236 cell line in presence of Nivolumab or IgG4 kappa isotype control antibody. Gating strategy for the assessment of immune checkpoint protein expression
B. Expression of PD1, LAG-3, TIM-3 and TIGIT in activated $CD4^+$ T cells alone and after overnight coculture with HRS cells from the L-1236 cell line in presence of Nivolumab or the IgG4 kappa isotype control antibody.
C. Expression of PD1, LAG-3, TIM-3 and TIGIT in activated $CD8^+$ T cells alone and after overnight coculture with HRS cells from the L-1236 cell line in presence of Nivolumab or the IgG4 kappa isotype control antibody.
D. Expression of PD1, LAG-3, TIM-3 and TIGIT in activated $CD4^+$ T cells after overnight coculture with HRS cells from a PD-L1 knockout L-1236 cell line or the L-1236 control cell line in presence of Nivolumab.
E. PD-L1 expression in the PD-L1 knockout L-1236 cell line and the L-1236 control cell line at baseline.

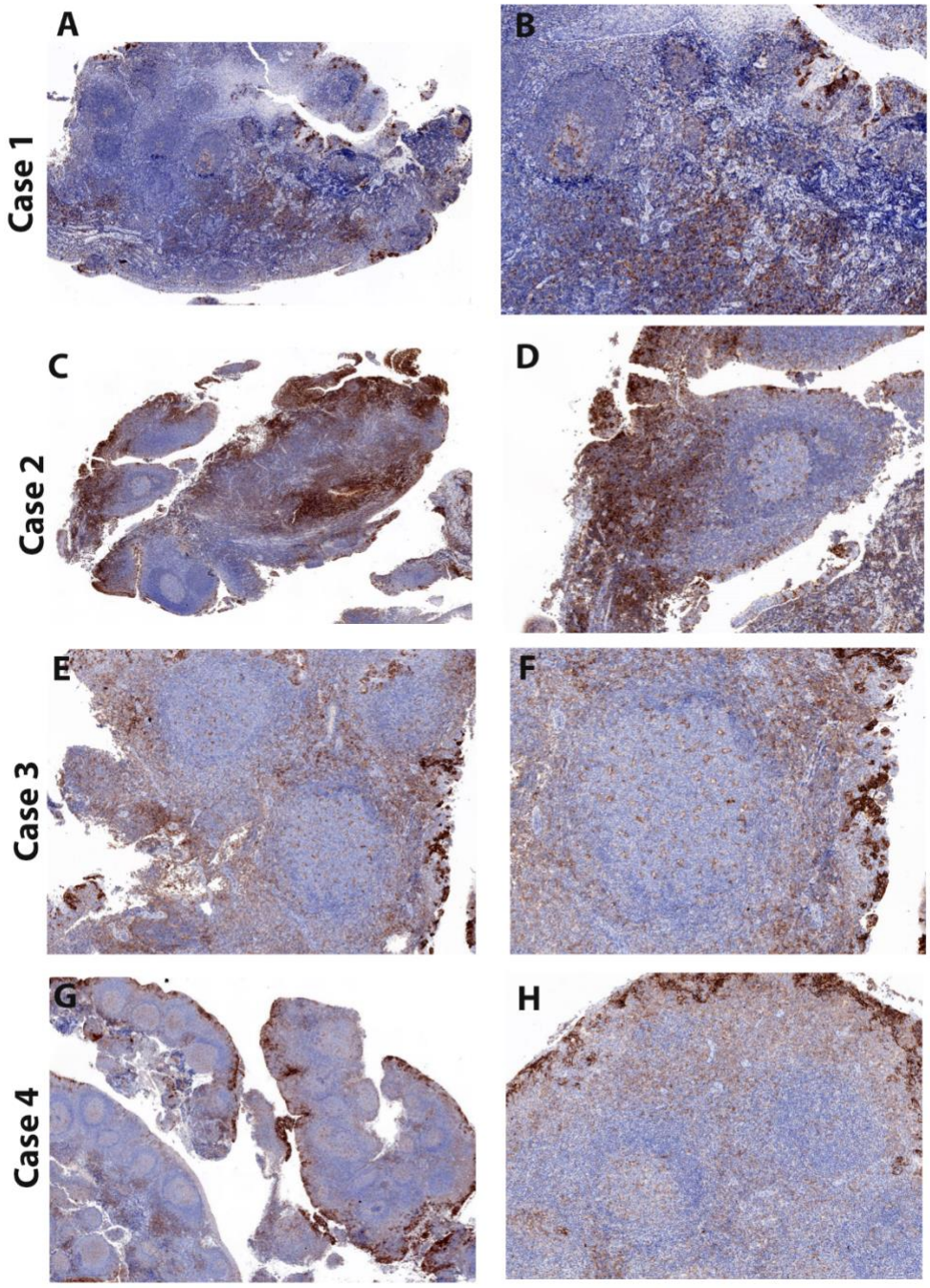

Suppl. Figure 5. PD-L1 expression in hyperplastic lymphatic tissue from the pharyngeal tonsil. Images from four representative of 13 donors.
A,C,E,G: 40-fold magnification of four representative examples of hyperplastic lymphoid tissue investigated by live cell imaging. B,D,F,H: 100-fold magnification of the same cases.

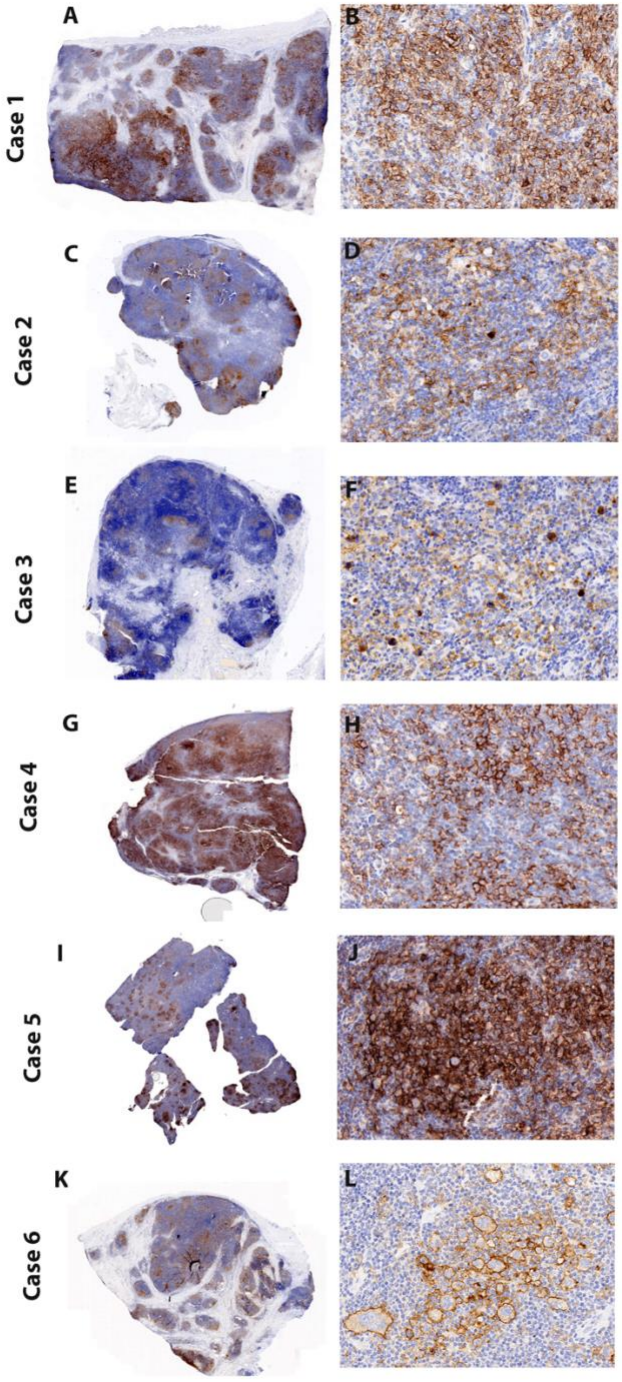

Suppl. Figure 6. PD-L1 expression in primary cases of classic Hodgkin lymphoma studied by live cell imaging.
A, C, E, G, I, K: 10-fold magnification of PD-L1 staining of the five cases investigated by live cell imaging.
B, D, F, H, J, L: 300-fold magnification of the same cases.

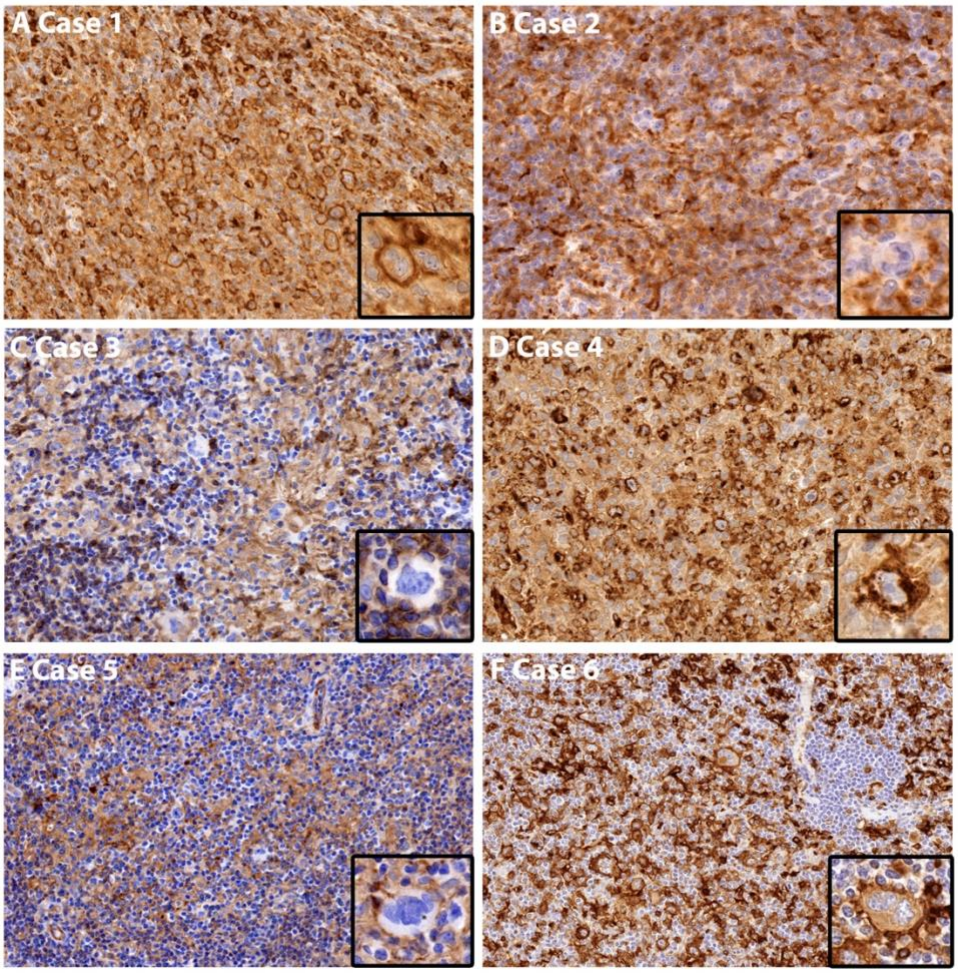

Suppl. Figure 7. MHC-II (HLA-DPB1) expression in the six classic Hodgkin lymphoma cases investigated by live cell imaging
A.-F. Cases 1-6 25 x magnification. Insert: Representative Hodgkin-Reed-Sternberg cells in 60x magnification.

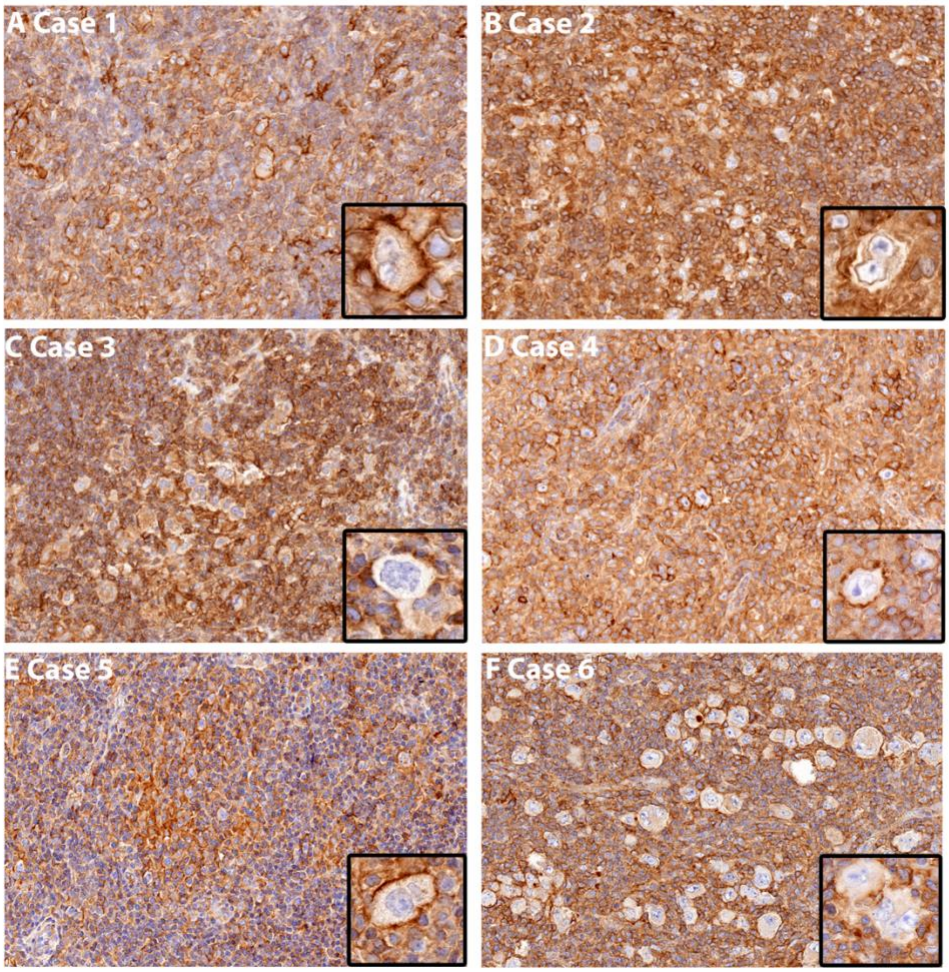

Suppl. Figure 8. MHC-I (HLA-ABC) expression in the six classic Hodgkin lymphoma cases investigated by live cell imaging
A.-F. Cases 1-6 25 x magnification. Insert: Representative Hodgkin-Reed-Sternberg cell in 60x magnification.

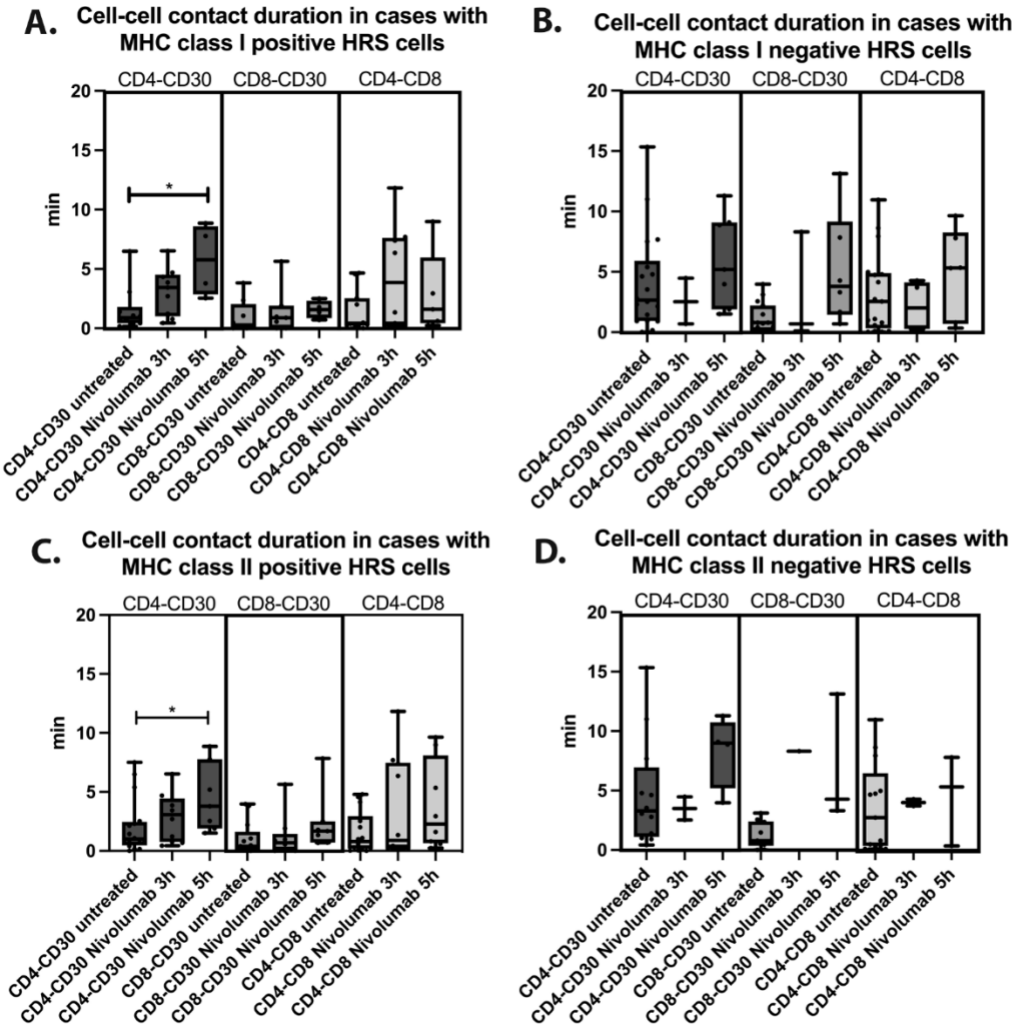

Suppl. Figure 9. Cell-cell contact duration according to MHC expression in Hodgkin-Reed-Sternberg (HRS) cells of the classic Hodgkin lymphoma cases investigated.

A. Cell-cell contact duration between $CD4^+$ T cells and HRS cells, $CD8^+$ T cells and HRS cells and $CD4^+$ and $CD8^+$ T cells in MHC I positive cHL cases (n= 3), each dot represents the mean of one movie
B. Cell-cell contact duration between $CD4^+$ T cells and HRS cells, $CD8^+$ T cells and HRS cells and $CD4^+$ and $CD8^+$ T cells in MHC I negative cHL cases (n= 3), each dot represents the mean of one movie
C. Cell-cell contact duration between $CD4^+$ T cells and HRS cells, $CD8^+$ T cells and HRS cells and $CD4^+$ and $CD8^+$ T cells in MHC II positive cHL cases (n= 3), each dot represents the mean of one movie

D. Cell-cell contact duration between $CD4^+$ T cells and HRS cells, $CD8^+$ T cells and HRS cells and $CD4^+$ and $CD8^+$ T cells in MHC II negative cHL cases (n= 3), each dot represents the mean of one movie

Suppl. Table 1. MHC I and II expression by immunohistochemistry in classic Hodgkin lymphoma cases investigated by live cell microscopy
NS: Nodular sclerosing subtype, MC: Mixed cellularity subtype

Case number	Subtype	MHC-I (HLA-ABC)	MHC-II (HLA-DPB1)
1	NS, EBV-	+	+
2	NS, EBV-	-	-
3	NS, EBV-	-	-
4	MC, EBV+	+	+
5	MC, EBV+	+	-
6	NS, EBV-	-	+

Supplementary Methods

Flow cytometry of classic Hodgkin lymphoma (cHL) cell lines

Non-transduced cHL cell lines were stained with antibodies against PD-L1 (Clone 29E.2A3 PE, Biolegend, San Diego, CA, USA), HLA-ABC (Clone G46-2.6, APC, ThermoFisher Scientific, Waltham, MA, USA) HLA-DR, DP, DQ (Clone Tu39 FITC, BD Biosciences,Heidelberg, Germany), and isotype controls and analyzed by fluorescence activated cell sorting (FACS) in a MACSQuant (Miltenyi Biotec, Bergisch Gladbach, Germany).

Cocultures of activated T cells with L-1236

After 48h of activation with dynabeads human T-Activator CD3/CD28 (Gibco, Thermofisher Scientific), activated $CD4^+$ or $CD8^+$ T cells were seeded in a 24-well plate with L-1236 cells (or L-1236 PD-L1 knockout cells) at a ratio of 20:1. Overnight culture was performed in the presence of Nivolumab or IgG4 isotype control antibody (10 µg/ml). After 24 h, cells were stained with either CD4-Vioblue or anti-CD8-Vioblue (both Miltenyi Biotec) and the following antibodies:
CD223 (LAG-3) Antibody, anti-human, APC, REAfinity (130-119-567), CD366 (TIM-3) Antibody, anti-human, APC, REAfinity (130-119-781), TIGIT Antibody, anti-human, APC, REAfinity (130-116-815), REA Control Antibody (S), human IgG1, APC, REAfinity (130-113-434, all Miltenyi), APC anti-human CD279 (PD-1) Antibody, clone EH12.2H7 (Biolegend) and Isotype APC Mouse IgG1, κ Isotype Ctrl Antibody MOPC-21 (both Biolegend).

Cells were gated on live population and the respective $CD4^+$ or $CD8^+$ T cell population and expression of the respective checkpoint proteins was assessed (Suppl. Figure 4A).

PD-L1 knockout L-1236 cell line

The PD-L1 knockout L-1236 cell line was obtained from Prof. Roland Schmitz, Gießen:

Vector construction

pLVX-TRE3G-Cas9-Hygro was created by removing the puromycin resistance gene from pLVX-TRE3G (Clontech Laboratories) with BfuAI/KpnI and replacing it with a synthetic Hygro construct. Cas9 was isolated using PCR from LentiCrispr v2 (Addgene #52961) and cloned into pLVX-TRE3G -Hygro digested with BamHI using Gibson cloning. SgRNA sequences targeting CD274 (ACATGTCAGTTCATGTTCAG) or AAVS1 control (GGGGCCACTAGGGACAGGAT) were cloned into pLenti guide dsRed (Addgene #128055) using BsmBI.

Generation of Doxycycline-inducible Cas9 expressing L-1236 clones

L-1236 cells were transduced with pLVX-Tet3G (Clontech Laboratories). 72 hours post-transduction, cells underwent selection with G418. Selected cells were transduced with pLVX-Tre3G-Cas9-Hygro. After 3 days of infection, transduced cells were split and incubated with hygromycin. A fraction of the selected pLVX-Tre3G-Cas9-Hygro cells were transduced with a sgRNA vector targeting nonessential surface markers such as ICAM1. 250 ng/mL of doxycycline was added to induce Cas9 and initiate genetic ablations for 8-11 days. The surface expression of the target gene was measured by FACS. After functional validation of Cas9, single-cell clones were generated by using limiting dilution from the pool of Cas9-expressing cells.

Lentivirus production and transduction

To generate lentivirus, HEK293FT cells (ThermoFisher) were cultured in DMEM medium supplemented with 10% FBS, 2 mM L-glutamine, and 1% penicillin-streptomycin. One day before transfection, HEK293FT cells were seeded in a 10 cm tissue culture dish at 60% confluency. Cells were transfected using TransIT-293 transfection reagent (Mirus). For each dish, 50 µl serum-free OptiMEM (Gibco) was mixed with 6 µg sgRNA vector, 4.5 µg psPax2 (Addgene #12260) and 1.5 µg pMD2.G (Addgene #12259). 27 µl TransIT-293 transfection reagent was diluted with 950µl OptiMEM, incubated for 5 min at room temperature, and combined with the mixture of plasmids. This transfection mixture was incubated for 30 min at room temperature and then added dropwise to the cells. Virus-containing supernatant was collected 72h post-transfection. Cell debris was removed by

centrifugation at 500xg for 10 min followed by filtration of the supernatant through a 0.45µm low-protein binding membrane (Millipore Steriflip HV/PVDF). Viral supernatant was concentrated by incubation with Lent-X concentrator (Takara) for at least 3h at 4°C. Virus was concentrated 100x, resuspended in sterile PBS, aliquoted, and frozen at -80°C. L-1236 doxycycline-inducible Cas9 cell line was transduced with lentivirus, and after 3 days of transduction, dsRed was measured using FACS. 250 ng/mL doxycycline was added for 8-11 days to induce Cas9. Cells were passaged every three days with fresh medium containing doxycycline and the surface expression of the targeted gene (CD274, clone 29E.2A3) was measured by FACS. Transduced post-doxycycline cells underwent two rounds of FACS sorting.